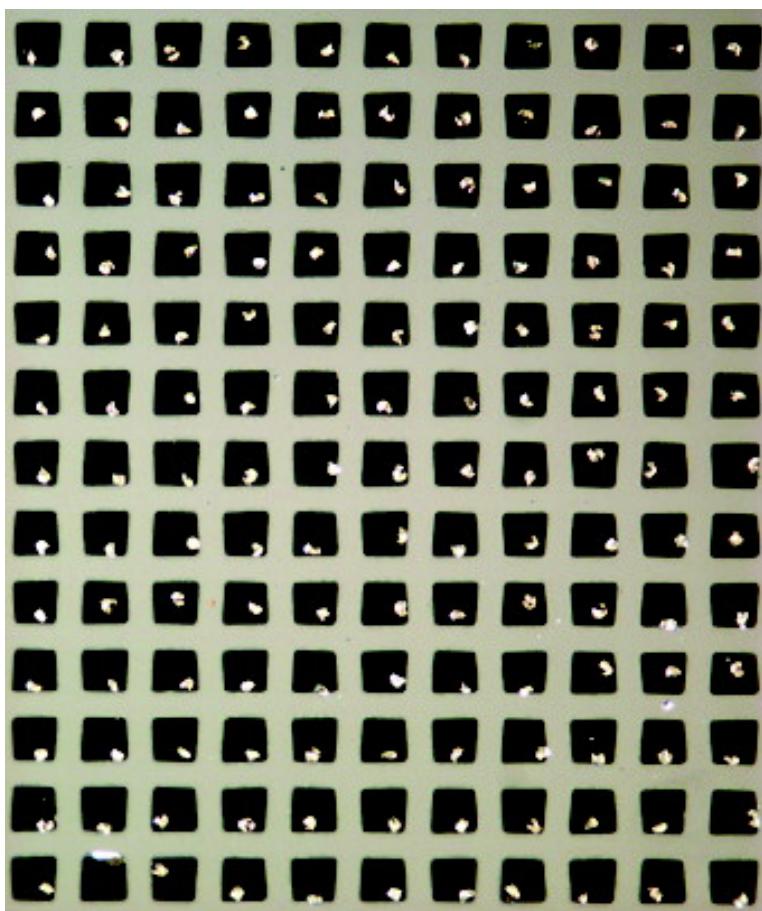


## Crystallization on Confined Engineered Surfaces: A Method to Control Crystal Size and Generate Different Polymorphs

Alfred Y. Lee, In Sung Lee, Severine S. Dette, Jana Boerner, and Allan S. Myerson

*J. Am. Chem. Soc.*, **2005**, 127 (43), 14982-14983 • DOI: 10.1021/ja055416x • Publication Date (Web): 07 October 2005

Downloaded from <http://pubs.acs.org> on March 25, 2009



### More About This Article

Additional resources and features associated with this article are available within the HTML version:

- Supporting Information



**ACS Publications**  
High quality. High impact.

- Links to the 12 articles that cite this article, as of the time of this article download
- Access to high resolution figures
- Links to articles and content related to this article
- Copyright permission to reproduce figures and/or text from this article

[View the Full Text HTML](#)



## Crystallization on Confined Engineered Surfaces: A Method to Control Crystal Size and Generate Different Polymorphs

Alfred Y. Lee,<sup>†</sup> In Sung Lee,<sup>†</sup> Severine S. Dette,<sup>†,‡</sup> Jana Boerner,<sup>†,‡</sup> and Allan S. Myerson<sup>\*,†</sup>

*Department of Chemical and Environmental Engineering, Illinois Institute of Technology, Chicago, Illinois 60616, and Institut fuer Verfahrenstechnik/TVT, Martin Luther Universitat Halle-Wittenberg, Hoher Weg 7, Halle/Saale, D-06099, Germany*

Received August 8, 2005; E-mail: myerson@iit.edu

In pharmaceutical product development, there has been an increased interest in the development of new drug delivery methods, particularly in the area of crystal size control and solid form purity. Current technologies, including crystallization-based methods and post-crystallization micronization processes (e.g. milling), can compromise the stability and properties of the drug material.<sup>1</sup> For instance, crystallization techniques to reduce the particle size such as supercritical fluid crystallization, impinging jet crystallization, solvent shifting, high pressure homogenization, and spray drying, depend on the generation of very high supersaturation, which favors nucleation over crystal growth.<sup>2</sup> Though these methods are successful in producing small particles, high supersaturation tends to cause the material to “oil-out” or phase separate, or leads to the formation of amorphous (noncrystalline) solids, or the production of an undesired crystal form, rather than the preferred polymorph.

Herein we describe a technique for the crystallization of micron size crystals of molecular organic compounds while operating at low and high supersaturations. The method is based on controlling the domain size available during the crystallization process. Patterned surfaces, specifically square metallic gold islands with self-assembled monolayers (SAMs) of lateral dimensions ranging from 25 to 725  $\mu\text{m}$ , serve as nucleation sites and are utilized to control the size of the crystals. Furthermore, the functionalized metallic islands can be used to screen polymorphs under different conditions. SAMs have been reported to serve as heterogeneous nucleants and can promote the nucleation and growth of organic,<sup>3,4</sup> inorganic,<sup>5</sup> and protein crystals.<sup>6</sup> Taking advantage of the surface chemistry that SAMs offer, hydrophilic (or lyophilic) gold islands surrounded by hydrophobic (or lyophobic) regions are created whereby wetting and dewetting of a liquid on the surface leads to formation of hemispherical droplets on the metallic islands.<sup>7</sup> The droplets contain the chemical of interest to be crystallized, and the size of the drops is dependent on the dimensions of the islands. As the arrays of droplets evaporate, crystallization occurs with the size of the particle dictated by the droplet size (or island size).

Metallic gold islands were formed by evaporation of titanium through a mesh onto glass slides, followed by a subsequent evaporation of gold through the stencil. The dimensions and patterns of the islands depend on the size and shape of the hole. Typically, the holes are shaped as squares. 4-Mercaptobenzoic acid (4-MBA) was selected as the thiol monolayers that self-assembled onto the gold surface, while octadecyltrichlorosilane (OTS) was used to backfill the glass-exposed substrate. The patterned bifunctional surface was immersed and slowly withdrawn from undersaturated aqueous solutions of glycine. The solution preferentially wets the metallic islands, and as the solvent evaporates, two-dimensional

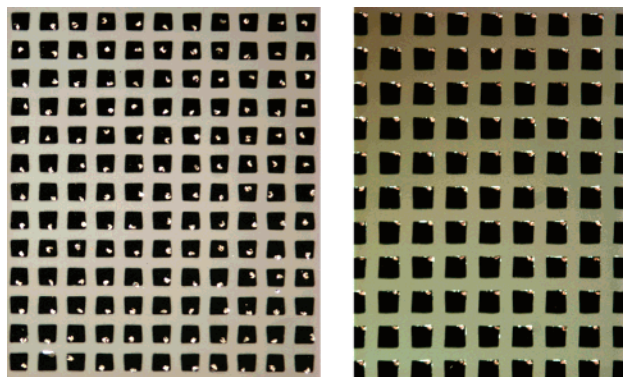


**Figure 1.** Patterned glycine crystals nucleated on 100  $\mu\text{m}$  (left) and 140  $\mu\text{m}$  (right) gold islands.

arrays of glycine crystals exclusively nucleate on the hydrophilic metallic islands.

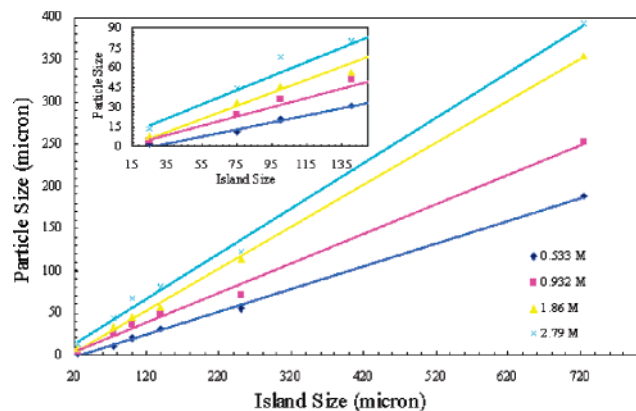
Glycine has three distinct solid-state phases:  $\alpha$ -,  $\beta$ -, and  $\gamma$ -forms. At ambient conditions,  $\gamma$ -glycine has the lowest free energy (or solubility) and is the thermodynamically stable form.<sup>8</sup> However, at higher temperatures,  $\gamma$ -glycine will transform to the  $\alpha$ -form as these modifications are enantiotropically related.  $\alpha$ -Glycine is typically produced from aqueous solution, while the  $\gamma$ -form can be obtained from acidic or basic solutions.<sup>9</sup>  $\beta$ -Glycine is the least stable form and is monotropically related to the other two phases. It can be obtained from an ethanol–water mixture and readily converts to the  $\alpha$ -modification in the presence of water or upon heating. More recently, two more solid forms ( $\delta$ - and  $\epsilon$ -forms) have been discovered under high pressure.<sup>10</sup>

Figure 1 shows the patterned crystallization of glycine from undersaturated aqueous glycine solutions on various feature sizes of metallic island substrates. On each island, a single leaf-shaped glycine crystal was observed with habits other than bipyramidal, needlelike, or triangle prism shapes, which are the typical crystal morphology for  $\alpha$ -,  $\beta$ -, and  $\gamma$ -glycine, respectively. The uniform array of glycine crystals that nucleated on the hydrophilic regions suggests that the drops were consistent and reproducible, and that the crystallization event on each island was homogeneous.

For a fixed solution concentration, the size of the particle is reduced as the area of the hydrophilic regions decreases as a result of the smaller drop volumes (Figure 2). The mean particle size on 725  $\mu\text{m}$  square islands for a 1.86 M glycine solution was 354.1  $\mu\text{m}$ , while the average lateral dimension on 25  $\mu\text{m}$  islands was 7.86  $\mu\text{m}$ . A 45-fold decrease was observed when the island size was reduced by a factor of almost 30. Furthermore, it was observed that the concentration of the solution can also affect the size of the crystals. Figure 2 describes the influence of solution concentration and the dimensions of the gold islands on the size of glycine

<sup>†</sup> Illinois Institute of Technology.

<sup>‡</sup> Martin Luther Universitat Halle-Wittenberg.



**Figure 2.** Effect of solution concentration and gold island size on the particle size of glycine.

**Table 1.** Glycine Polymorph Distribution for Different Gold Island Sizes (The Color of Each Row Represents the Number of Crystals Analyzed: 50-Yellow; 75-Green; and 100-Blue)

Island Size	1.86 M Solution			Maximum Error	2.79 M Solution			Maximum Error
	$\alpha$ -form	$\beta$ -form	$\gamma$ -form		$\alpha$ -form	$\beta$ -form	$\gamma$ -form	
725 $\mu\text{m}$	100.0	0.0	0.0	0.000	94.0	0.0	6.0	0.018
250 $\mu\text{m}$	72.0	24.0	4.0	0.113	94.0	6.0	0.0	0.063
140 $\mu\text{m}$	68.0	32.0	0.0	0.127	88.0	12.0	0.0	0.088
100 $\mu\text{m}$	56.0	44.0	0.0	0.111	50.7	46.6	2.7	0.112
25 $\mu\text{m}$	0.0	100.0	0.0	0.000	11.0	89.0	0.0	0.061

crystals. As the solution concentration increases for a particular square island, the size of the crystals increases as well. This is not surprising considering that there is an increase in the relative amounts of glycine molecules in the droplets compared to the dilute drops since there is additional solute to attach onto the growing surface of the crystals.

Raman microscopy is employed to identify the polymorphic forms of glycine for crystals that nucleated on the hydrophilic square islands. Reference Raman spectra for each form of glycine were collected, and comparison of the peak positions enabled us to discriminate the crystal modifications on each island. The Raman spectra of the three crystal forms of glycine collected over a range of 200 to 3200  $\text{cm}^{-1}$  can be found in the Supporting Information. The Raman spectra are considerably different as certain bands shifted to higher or lower wavenumbers. For instance, the  $\text{CH}_2$  symmetric stretch mode for  $\alpha$ -glycine is at 2972  $\text{cm}^{-1}$ ; however, for  $\beta$ - and  $\gamma$ -glycine, the band shifts lower to 2953 and 2964  $\text{cm}^{-1}$ , respectively.

Table 1 summarizes the polymorph distribution of glycine crystals on various metallic island sizes. On large hydrophilic gold islands (725  $\mu\text{m}$ ),  $\alpha$ -glycine predominately crystallized from aqueous solution. As the feature size of the metallic island decreases, the appearance of  $\alpha$ -glycine crystals declines while the number of  $\beta$ -form crystals steadily rises from 0% on 725  $\mu\text{m}$  square islands to almost 90% or higher on 25  $\mu\text{m}$  square islands. In two instances, all three solid phases simultaneously appeared.

The concomitant crystallization of glycine from aqueous solution and the increased frequency of the high energy form ( $\beta$ -glycine) with decreasing feature sizes is a result of the high supersaturation that is generated from the fast solvent evaporation. As the volume of the droplets decreases (from microliters to nanoliters), the rate of evaporation increases, whereby the array of aqueous solution droplets becomes highly supersaturated and metastable with respect to the  $\beta$ -phase. Consequently, this high energy kinetic form is energetically favored. On several occasions,  $\gamma$ -glycine was also observed. This is not surprising considering that the  $\gamma$ -form can

grow from heavy water solutions, which lends support to Iitaka's comments that glycine crystallizes in many forms, even unstable ones in aqueous solutions.<sup>9</sup> It is likely that the  $\gamma$ -form might have crystallized on the other island dimensions but was not detected due to the small sample size of characterized crystals. In several cases, the estimated errors are reasonably high, suggesting that there are uncertainties and additional crystals are required for Raman analysis in order to obtain a better statistical description of the concomitant nucleation of glycine polymorphs.

SAMs can direct the polymorph selectivity of organic<sup>4</sup> and inorganic<sup>5</sup> crystals. However, it is observed that 4-MBA SAMs template the oriented nucleation of  $\alpha$ -glycine with the {121} crystallographic surface corresponding to nucleation. The fact that the concomitant polymorphs become biased toward the least stable phase at smaller metallic island sizes suggests that the polymorphic outcome is primarily influenced by other factors, namely, the solvent evaporation rate.

In summary, patterned metallic gold islands are fabricated and utilized as a new method for particle engineering. This bottom-up approach involves the nucleation and growth of organic molecular crystals on hydrophilic (or lyophilic) square islands surrounded by hydrophobic (or lyophobic) regions. Crystallization is confined to the metallic islands as the size and area of the particle can be controlled by varying the feature size of the islands or the concentration of the solution. This technique has the potential to lead to the generation of nanometer size crystals as the domain size available during crystallization can be further reduced. Additionally, fast solvent evaporation in the drops can lead to high supersaturation, where high energy metastable polymorphs are energetically favored and can nucleate and grow. Lastly, given that different polymorphic forms are obtained on the identical islands under the same conditions, crystallization in constrained environments<sup>11</sup> can aid in understanding the concomitant nucleation of polymorphs and can have a significant impact on the development of new crystallization protocols.

**Acknowledgment.** This work was funded by the U.S. Army Medical Research and Materiel Command (W81XWH0410864). We are grateful to Professor Victor H. Perez-Luna for providing access to the electron beam evaporator.

**Supporting Information Available:** Raman spectra of the different polymorphs of glycine. This material is available free of charge via the Internet at <http://pubs.acs.org>.

## References

- (1) Brittain, H. G. *J. Pharm. Sci.* **2002**, *91*, 1573.
- (2) Mahajan, A. J.; Kirwan, D. J. *J. Phys. D: Appl. Phys.* **1993**, *26*, B176.
- (3) (a) Frostman, L. M.; Bader, M. M.; Ward, M. D. *Langmuir* **1994**, *10*, 576. (b) Lee, A. Y.; Ulman, A.; Myerson, A. S. *Langmuir* **2002**, *18*, 5886.
- (4) (a) Carter, P. W.; Ward, M. D. *J. Am. Chem. Soc.* **1994**, *116*, 769. (b) Hiremath, R.; Varney, S. W.; Swift, J. A. *Chem. Commun.* **2004**, 2676.
- (5) Aizenberg, J.; Black, A. J.; Whitesides, G. M. *J. Am. Chem. Soc.* **1999**, *121*, 4500.
- (6) Pham, T.; Lai, D.; Ji, D.; Tuntivechapiikul, W.; Friedman, J. M.; Lee, T. R. *Colloids Surf., B* **2004**, *34*, 191.
- (7) Kumar, A.; Whitesides, G. M. *Science* **1994**, 263, 60.
- (8) Boldyreva, E. V.; Drebushchak, V. A.; Drebushchak, T. N.; Paukov, I. E.; Kovalevskaya, Y. A.; Shutova, E. S. *J. Therm. Anal. Cal.* **2003**, *73*, 409.
- (9) Iitaka, Y. *Acta Crystallogr.* **1961**, *14*, 1.
- (10) Dawson, A.; Allan, D. R.; Belmonte, S. A.; Clark, S. J.; David, W. I. F.; McGregor, P. A.; Parson, S.; Pulham, C. R.; Sawyer, L. *Cryst. Growth Des.* **2005**, *5*, 1415.
- (11) (a) Ha, J. M.; Wolf, J. H.; Hillmyer, M. A.; Ward, M. D. *J. Am. Chem. Soc.* **2004**, *126*, 3382. (b) Thalladi, V. R.; Whitesides, G. M. *J. Am. Chem. Soc.* **2002**, *124*, 3520. (c) Hilden, J. L.; Reyes, C. E.; Kelm, M. J.; Tan, J. S.; Stowell, J. G.; Morris, K. R. *Cryst. Growth Des.* **2003**, *3*, 921.

JA055416X